

---

# Sequential Encryption of Sparse Neural Networks Toward Optimum Representation of Irregular Sparsity

---

Baeseong Park<sup>\*1</sup> Se Jung Kwon<sup>\*1</sup> Dongsoo Lee<sup>\*1</sup> Daehwan Oh<sup>1</sup> Byeongwook Kim<sup>1</sup> Yongkweon Jeon<sup>1</sup>  
Yeonju Ro<sup>1</sup>

## Abstract

Even though fine-grained pruning techniques achieve a high compression ratio, conventional sparsity representations (such as CSR) associated with irregular sparsity degrade parallelism significantly. Practical pruning methods, thus, usually lower pruning rates (by structured pruning) to improve parallelism. In this paper, we study fixed-to-fixed (lossless) encryption architecture/algorithm to support fine-grained pruning methods such that sparse neural networks can be stored in a highly regular structure. We first estimate the maximum compression ratio of encryption-based compression using entropy. Then, as an effort to push the compression ratio to the theoretical maximum (by entropy), we propose a sequential fixed-to-fixed encryption scheme. We demonstrate that our proposed compression scheme achieves almost the maximum compression ratio for the Transformer and ResNet-50 pruned by various fine-grained pruning methods.

## 1. Introduction

As neural networks (NNs) become larger and deeper to achieve higher model accuracy, various model compression techniques have been developed to compress NNs without compromising accuracy. As one of the efficient compression methods, pruning reduces the number of parameters by replacing model parameters of low importance with zeros (LeCun et al., 1990). Since magnitude-based pruning has shown that pruning can be conducted with low computational complexity (Han et al., 2015), various practical pruning methods have been studied to achieve higher compression ratio (Zhu & Gupta, 2017; Molchanov et al., 2017; Louizos et al., 2018; Gale et al., 2019). Recently, pruning

has been extended to a deeper understanding of weight initialization. Based on the *Lottery Winning Ticket* hypothesis (Frankle & Carbin, 2018), (Renda et al., 2020) suggests a weight-rewinding method to explore sub-networks from full-trained models. Furthermore, pruning at initialization steps without pre-trained models, such as SNIP (Lee et al., 2019b) and GraSP (Wang et al., 2020), has also been proposed.

Despite a high compression ratio, fine-grained pruning that eliminates each parameter individually has practical issues to be employed in parallel computing platforms. One of the popular formats to represent sparse matrices after pruning is the Compressed Sparse Row (CSR) whose structures are irregular. For parallel computing, such irregular formats degrade inference performance that is dominated by matrix multiplications (Gale et al., 2020). For example, performance gain using a sparse matrix multiplication (based on CSR) is a lot smaller than the compression ratio of pruning (Yu et al., 2017). Moreover, it should be noted that **a sparse matrix multiplication can be even slower than a dense matrix multiplication unless pruning rate is high enough** (Yu et al., 2017; Gale et al., 2020) that does not happen if a regular format maintaining parallelism is available after pruning.

Structured pruning methods (e.g. block-based pruning (Narang et al., 2017; Zhou et al., 2021), filter-based pruning (Li et al., 2017), and channel-based pruning (He et al., 2017; Liu et al., 2017)) have been suggested to enhance parallelism by restricting the locations of pruned weights. Those methods, however, induce degraded accuracy and/or lower pruning rate than fine-grained (unstructured) pruning.

In this paper, as an efficient method to compress sparse NNs pruned by fine-grained pruning, we consider weight encryption techniques. We study the maximum compression ratio of such encryption-based compression using entropy and propose a sequential fixed-to-fixed scheme that keeps high parallelism after fine-grained pruning. We show that by our proposed fixed-to-fixed scheme, a compression ratio can approach the maximum (estimated by entropy) even under the variation of the unpruned weights in a block.

---

<sup>\*</sup>Equal contribution <sup>1</sup>Samsung Research, Seoul, Republic of Korea. Correspondence to: Baeseong Park <bpbs.park@samsung.com>.

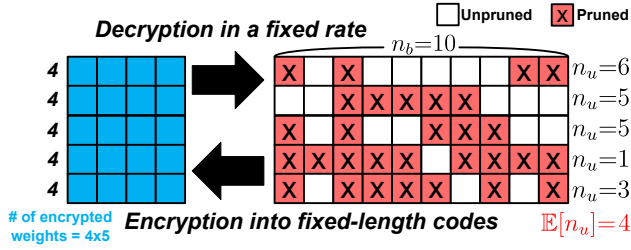


Figure 1. Fixed-to-fixed compression of a sparse weight matrix. Even when a block involves a varying number of unpruned weights, the size of each encrypted block is fixed and determined by an average number of unpruned weights in blocks.

## 2. Fixed-to-Fixed Sparsity Encryption

Data compression is a process of encoding (or encrypting) original data into a smaller size. If a fixed number of original bits are encrypted into a fixed number of (smaller) bits, such a case is categorized into a “fixed-to-fixed” compression scheme. Similarly, “fixed-to-variable”, “variable-to-fixed”, and “variable-to-variable” categories are available while variable lengths of original and/or encrypted bits allow higher compression ratio than fixed ones (e.g., Huffman codes (Huffman, 1952) as fixed-to-variable scheme, Lempel-Ziv (LZ)-based coding (Ziv & Lempel, 2006) as variable-to-fixed scheme, and Golomb codes (Golomb, 1966) as variable-to-variable scheme).

Among those 4 categories, “fixed-to-fixed” compression is the best for NNs that rely on parallel computing systems. Fixed-to-fixed schemes are, however, challenging when fine-grained pruning is employed in NNs because the number of unpruned weights in a fixed-size block varies. Accordingly, most previous sparsity representations (such as CSR format) translate a fixed-size weight block into a variable-size block while such a translation would demand non-uniform memory accesses that lead to significantly degraded memory bandwidth utilization. In this work, we consider a “fixed-to-fixed” compression scheme as shown in Figure 1 when the number of pruned weights in a block can vary. A successful fixed-to-fixed compression of sparse NNs should consider the followings:

- **(High compression ratio)** As we discuss later, the maximum compression ratio is limited by the minimum entropy (that can be obtained by a fixed-to-variable scheme). Suppose that a block to be encrypted contains (fixed)  $n_b$  bits among which (fixed)  $n_u$  bits are unpruned. A fixed-to-fixed encryption scheme is required to support high compression close to  $(n_b/n_u)$  (estimated by entropy). Fixed-to-fixed decryption, then, accepts (fixed)  $N_{in}$  bits as an input and produces  $N_{out}$  bits as an output while  $N_{out}/N_{in} =$

$$n_b/n_u.$$

- **(Variation tolerance)** For a fine-grained pruning,  $n_u$  is given as a random variable whose distribution is affected by pruning rate,  $n_b$  size, a particular pruning method, and so on. Our goal is to maintain a fixed-to-fixed scheme with a high compression ratio even under  $\text{Var}[n_u] \neq 0$ . In Figure 1, for example, 5 blocks of original data have various  $n_u$  values while the size of an encoded block is fixed to be 4 ( $=\mathbb{E}[n_u]$ ). We will discuss how to design a variation tolerant encryption.

## 3. Fundamental Limits of Compression

Before we suggest a fixed-to-fixed compression scheme, we are interested in the upper bound of compression ratio that can be analyzed by entropy assuming fixed-to-variable compression. Then, when we suggest a fixed-to-fixed compression scheme, we can estimate how close the compression capability of a fixed-to-fixed scheme is to the maximum.

Entropy presents the minimum average number of bits to represent an event when a probability distribution of those events is provided (Morelos-Zaragoza, 2006). To investigate the entropy of pruned weight blocks (and the maximum compression ratio correspondingly), a block of bits is assigned to a symbol such that a probability distribution of symbols minimizes the entropy. In other words, symbol assignment is designed to minimize the average number of bits (i.e., entropy to represent symbols) that is given as

$$H = - \sum_{i=1}^n p_i \cdot \log_2 p_i, \quad (1)$$

where  $n$  is the total number of symbols and  $p_i$  is the occurrence probability of each symbol.

Before we discuss such a symbol assignment method, let us assume that a binary masking matrix is given to represent which weights are pruned or not (note such a binary masking matrix can be compressed significantly (Lee et al., 2019a)). Then, a pruned weight can be described as a don’t care value (X) that is to be masked. To study the limits of compression ratio, we also assume that 1) pruning each weight is performed independently with pruning rate  $S$  and 2) unpruned weight is assigned to 0 or 1 with equal probability.

**Symbol assignment** We concatenate all of  $k$ -th bits of weights into a group and produce  $n_w$  groups when  $n_w$  is the number of bits to represent a weight (e.g.,  $n_w$  is 32 for single-precision and 8 for INT8) and  $1 \leq k \leq n_w$ . Symbol assignment is performed in each group independently without referring to other groups. Suppose that a certain

block from one of the groups is given as  $\{0\times\times 1\}$  and corresponding mask bits (that are shared by all  $n_w$  groups) are  $\{1001\}$  (0 means masking). By filling up  $\times$  with 0 or 1,  $\{0\times\times 1\}$  is selected to be assigned to one of 4 symbols (i.e.,  $\{0001\}$ ,  $\{0011\}$ ,  $\{0101\}$  or  $\{0111\}$ ) while such a symbol selection decides entropy. In the following two examples (where  $n_b=4$ ), we illustrate the symbol assignment method that minimizes the entropy.

**Entropy ( $n_u = 1$ , e.g.,  $\{\times\times\times 0\}$ ,  $\{\times 1\times\times\}$ )** In this case, every block (of  $n_b=4$  and  $n_u=1$ ) can be assigned to either one of two symbols ( $\{0000\}$ ,  $\{1111\}$ ). Since  $P(0000) = P(1111) = 0.5$ , from Eq. 1,  $H = -(0.5 \times (-1) + 0.5 \times (-1)) = 1$ . Thus, a block of  $n_b=4$  and  $n_u=1$  can be compressed into 1 bit that indicates one of two symbols. There are many other sets of two symbols to meet  $H = 1$ , such as ( $\{0010\}$ ,  $\{1101\}$ ) and ( $\{1010\}$ ,  $\{0101\}$ ).

**Entropy ( $n_u = 2$ , e.g.,  $\{\times 01\times\}$ ,  $\{10\times\times\}$ )** A set of symbols should meet the following requirement: if we choose random  $n1$  and random  $n2$  ( $1 \leq n1, n2 \leq n_b, n1 \neq n2$ ) and collect  $\{n1\text{-th bit}, n2\text{-th bit}\}$  of each symbol, then, each of  $\{00, 01, 10, 11\}$  should appear in the collection. Under such a constraint, after a careful investigation using a full search, the minimum number of symbols is 5 to represent all blocks of  $n_b=4$  and  $n_u=2$ . An example set of 5 symbols with corresponding occurrence probability to minimize entropy is as follows:  $P(0000) = 6/24$ ,  $P(1110) = 6/24$ ,  $P(0101) = 5/24$ ,  $P(1001) = 4/24$ , and  $P(0011) = 3/24$ . Then, from Eq. 1,  $H$  is approximately 2.28 (bits) attainable through fixed-to-variable compression. On the other hand, for a fixed-to-fixed scheme, a block (of  $n_b=4$  and  $n_u=2$ ) is compressed into 3 bits to represent one of 5 symbols.

For  $n_u=3$ , the minimum number of symbols is 8 and a block can be compressed into 3 bits. We can generalize various  $n_u$  cases: **when  $n_u$  is fixed across blocks,  $H$  can be equal to or slightly higher than  $n_u$ .**

#### 4. Random Number Generator

While entropy can provide the upper limit of compression ratio, a compression scheme based on the principles of entropy has some practical issues because 1) entropy assumes a fixed-to-variable compression scheme while we are interested in a fixed-to-fixed scheme, and 2) symbols and corresponding index data need to be stored in a look-up table that grows exponentially with entropy. Hence, instead of symbol assignment and entropy, we consider encryption methods using a random number generator.

A random number generator accepts a fixed number of inputs and produces  $n_b$  bits so as to implement a fixed-to-fixed compression scheme. As shown in Figure 2, a weight

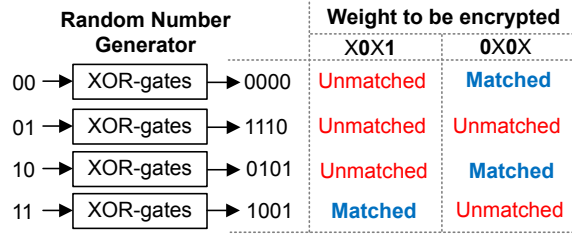


Figure 2. Encryption of weights using an XOR-gate network as a random number generator.

block is compared with every output of a random number generator. If there is an output vector matching original (masked) weights, then a corresponding input vector of a random number generator can be an encrypted input vector. As an effort to increase the Hamming distance between any two outputs (i.e., the number of bit positions in which two bits are different),  $2^{n_u}$  outputs out of  $2^{n_b}$  possible candidates need to be randomly selected. Note that random encryption has already been suggested by Claude Shannon to introduce channel capacity that is the fundamental theory in digital communication (Morelos-Zaragoza, 2006). Since then, practical error correction coding techniques have been proposed to implement random-like coding by taking into account efficient decoding (instead of using a large look-up table).

Similar to error correction coding that usually depends on linear operations over Galois Field with two elements ( $GF(2)$ ) for simple encryption of original data, recently, two compression techniques for sparse NNs have been proposed. An XOR-gate network produces (a large number of) binary outputs using (a relatively much smaller number of) binary inputs while outputs are quantized weights (Kwon et al., 2020). Another example is to adopt a Viterbi encoding/decoding scheme (Forney, 1973) to generate multiple bits using a single bit as an input (Ahn et al., 2019). For a block that cannot be encrypted into a compressed one by a random number generator, we can attach patch data to fix unmatched bits (Kwon et al., 2020) or re-train the model to improve the accuracy (Ahn et al., 2019).

To compare the random number generation capability of various block-level compression schemes, we introduce ‘encryption efficiency’ given as a percentage.

#### Encryption efficiency ( $E$ )

$$E = \frac{\# \text{ of correctly matched bits}}{\# \text{ of unpruned bits}} \times 100(\%) \quad (2)$$

Let  $S$  be pruning rate ( $0 \leq S \leq 1$ ). To measure encryption efficiency ( $E$ ), we assume that the compression ratio of a random number generator (=the number of output bits

$N_{in}$	$S$					$N_{in}$	$S$					$N_{in}$	$S$				
	0.5	0.6	0.7	0.8	0.9		0.5	0.6	0.7	0.8	0.9		0.5	0.6	0.7	0.8	0.9
4	90.03 (±7.03)	89.98 (±6.85)	89.48 (±7.41)	90.35 (±3.80)	90.24 (±2.51)	4	88.24 (±7.23)	88.46 (±6.17)	88.32 (±5.44)	87.82 (±4.31)	87.67 (±2.33)	4	88.31 (±7.19)	88.07 (±6.09)	87.16 (±5.49)	86.91 (±4.39)	86.67 (±3.03)
8	94.99 (±2.28)	95.02 (±1.54)	95.34 (±1.29)	95.07 (±0.82)	95.00 (±0.81)	8	94.12 (±1.51)	93.72 (±1.43)	93.91 (±1.21)	93.46 (±1.10)	93.22 (±0.90)	8	93.75 (±1.67)	93.19 (±1.38)	93.00 (±1.03)	92.61 (±1.01)	92.39 (±0.60)
12	96.75 (±0.68)	96.74 (±0.41)	97.06 (±0.54)	96.72 (±0.35)	96.72 (±0.35)	12	95.86 (±0.83)	95.78 (±0.45)	95.91 (±0.75)	95.43 (±0.32)	95.36 (±0.35)	12	95.59 (±0.67)	95.23 (±0.72)	94.89 (±0.50)	94.71 (±0.33)	94.50 (±0.28)
16	97.53 (±0.36)	97.55 (±0.21)	97.65 (±0.17)	97.55 (±0.36)	97.57 (±0.31)	16	96.82 (±0.32)	96.71 (±0.22)	96.68 (±0.25)	96.52 (±0.19)	96.41 (±0.26)	16	96.43 (±0.36)	96.18 (±0.25)	95.69 (±0.13)	95.73 (±0.12)	95.56 (±0.16)
20	98.05 (±0.18)	98.06 (±0.12)	98.19 (±0.14)	98.05 (±0.17)	98.05 (±0.26)	20	97.44 (±0.13)	97.28 (±0.15)	97.32 (±0.14)	97.12 (±0.17)	97.03 (±0.24)	20	97.08 (±0.12)	96.79 (±0.09)	96.32 (±0.08)	96.40 (±0.08)	96.35 (±0.13)

(a)  $n_u$  (=a number of unpruned weights in a block) is fixed to be  $N_{in}$  (i.e.,  $B(N_{out}, 1-S)$ ,  $\text{Var}[n_u]=0$ ). (b)  $n_u$  follows a binomial distribution. (c)  $n_u$  is empirically obtained by pruning the first decoder layer of the Transformer using a magnitude-based pruning method.

Figure 3. Encryption efficiency (%) of random XOR-gate networks.  $S$  is entire pruning rate and  $N_{out}$  is given as  $\lfloor N_{in} \cdot (1/(1-S)) \rfloor$ .

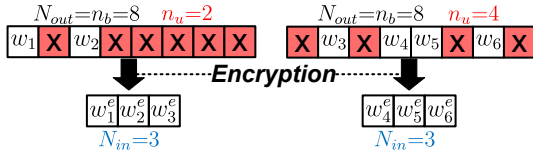


Figure 4. Encryption of two blocks when a number of unpruned weights can vary in a block.

/ the number of input bits) is  $1/(1-S)$ . We generate numerous randomly pruned (binary) weight blocks, and for each block, we investigate all of the possible outputs that a random number generator can produce. If there is a block missing a matching output of a generator, then the maximum number of correctly matched bits is recorded for each block. We repeat such an experiment for all of the blocks. Since the number of encrypted bits cannot be smaller than the number of unpruned bits as we discussed with entropy,  $E$  cannot be higher than 100% for any generators.

#### 4.1. Fixed Pruning Rate in a Block

For simplicity, we assume that  $n_u$  in a block is a fixed number. Let us study  $E$  when  $n_u$  is fixed using an XOR-gate network introduced in (Kwon et al., 2020). For an XOR-gate network, when  $N_{out}$  is the number of output bits and  $N_{in}$  is the number of input bits, a matrix  $M^\oplus \in \{0, 1\}^{N_{out} \times N_{in}}$  presents connectivity information between an input vector  $w^x \in \{0, 1\}^{N_{in}}$  and an output vector  $w^y \in \{0, 1\}^{N_{out}}$  such that we have  $w^y = M^\oplus \cdot w^x$  over  $GF(2)$ . For example, if the second row of  $M^\oplus$  (with  $N_{in} = 4$  and  $N_{out} = 8$ ) is given as  $[1011]$ , then  $w_2^y = w_1^x \oplus w_3^x \oplus w_4^x$  ( $\oplus$  indicates a binary XOR operation or an addition over  $GF(2)$  equivalently). An element of  $M^\oplus$  is randomly filled with 0 or 1 as a simple random number generator design technique (Kwon et al., 2020).

To measure  $E$ , let  $N_{in}/N_{out} \approx 1-S$  such that  $N_{out} =$

$\lfloor N_{in} \cdot (1/(1-S)) \rfloor$ . Correspondingly, for a certain  $S$ , a block size (=  $N_{out}$ ) increases as  $N_{in}$  increases. When  $n_b = N_{out}$  and  $n_u = N_{in}$ , Figure 3a describes statistics of  $E$  when random  $M^\oplus$  matrices are associated with random blocks. From Figure 3a, it is clear that increasing  $N_{in}$  is the key to improving encryption efficiency. Note that, however, increasing  $N_{in}$  and  $N_{out}$  complicates the decryption complexity (due to large  $M^\oplus$ ) and the encryption complexity as well (due to an exponentially large search space).

#### 4.2. Variable Pruning Rate in a Block

Now we allow  $n_u$  in a block to fluctuate. For Figure 3b, we assume that pruning each weight is a Bernoulli event (with  $S$  probability) such that  $n_u$  in a block follows a binomial distribution  $B(N_{out}, 1-S)$  (thus,  $\mathbb{E}[n_u] = N_{out}(1-S)$  and  $\text{Var}[n_u] = N_{out}S(1-S)$ ).  $N_{in}$  is given as  $\mathbb{E}[n_u]$  in Figure 3b. Compared to Figure 3a, we observe that  $E$  becomes lower mainly because some blocks would have  $n_u$  larger than  $N_{in}$  (i.e., too many unpruned weight bits that a random number generator cannot target).

Note that the coefficient of variation of  $n_u$  ( $=\sqrt{\text{Var}[n_u]}/\mathbb{E}[n_u] = \sqrt{S/(N_{out}(1-S))}$ ) decreases as  $N_{out}$  increases. Indeed, the gap between  $E$  in Figure 3a and  $E$  in Figure 3b tends to be slightly reduced when  $N_{in}$  (as well as corresponding  $N_{out}$ ) increases. To illustrate, as shown in Figure 4, when there are two blocks of different  $n_u$ , concatenating two blocks into a block (thus, increasing  $N_{out}$ ) can increase the probability of successful encryption due to efficient usage of  $N_{in}$ . Increasing  $N_{in}$  and  $N_{out}$  by  $n$  times, however, requires an XOR-gate network to be larger by  $n^2$  times with only a marginal gain in  $E$ .

Another way to improve  $E$  under the variation on  $n_u$  is to decrease  $N_{out}$  and increase  $N_{in}$ . In this case, however, the compression ratio is reduced consequently. We need a solution to design a fixed-to-fixed sparsity compression technique that can improve  $E$  of a random number generator under the variation on  $n_u$  without sacrificing compression





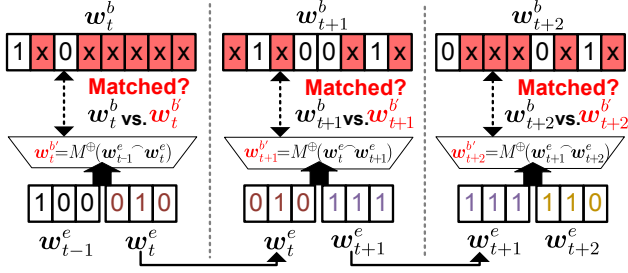


Figure 6. Sequential decryption example when  $N_s=1$ ,  $N_{in}=3$ , and  $N_{out}=8$ . An input vector is utilized for 2 ( $=N_s+1$ ) time indices through shift registers.

**Balanced encryption** Figure 6 illustrates a decryption process when  $N_s=1$ ,  $N_{in}=3$ , and  $N_{out}=8$ . Each weight vector to be encrypted contains a different number of unpruned weights. For  $w_t^{b'}$  at time index  $t$  (in Figure 6), a less number of unpruned weights tends to enlarge search space for  $w_t^e$ . On the other hand for  $w_{t+1}^{b'}$  at time index  $(t+1)$ , a large number of unpruned weights would highly restrict search space for  $w_t^e$ . Correspondingly, compared to the case when  $w_t^e$  is associated with only one  $w^{b'}$  block (i.e., non-sequential encryption with  $N_s=0$ ), search space for  $w_t^e$  can be balanced as more  $w^{b'}$  blocks of various  $n_u$  are correlated with  $w_t^e$ . Note that as  $\text{Var}[n_u]$  of one block increases, according to the central limit theorem,  $N_s$  is required to be larger to maintain the balance of encryption capability of each  $w_t^e$ . As we demonstrate in the next section, under the variation on  $n_u$ , even small non-zero  $N_s$  can enhance  $E$  substantially while increasing  $N_{in}$  (and  $N_{out}$  while  $N_s=0$ ) improves  $E$  only marginally (as described in Figure 3).

**Encryption algorithm** In the case of a non-sequential encryption scheme, because of one-to-one correspondence between  $w_t^e$  and  $w_t^{b'}$  through  $M^{\oplus}$ , encryption can be performed independently for each block (e.g., for a given masked  $w_t^b$ , we select one matching  $w_t^{b'}$  out of all available  $w_t^{b'}$  sets by a decryptor). Such block-wise encryption, however, is not applicable to a sequential encryption scheme that needs to consider the whole sequence of  $w^b$  blocks to find an input sequence fed into a decryptor. Suppose that we find a particular output sequence matching  $l$  blocks after exploring all feasible output sequences provided by a generator and the input sequence  $(w_1^e, w_2^e, \dots, w_l^e)$ , the time- and space-complexity of encryption would be  $\mathcal{O}(2^{N_{in} \cdot l})$ . Fortunately, sequential decryption operations shown in Figure 6 can be modeled as a hidden Markov model, where each state is represented by concatenating  $w_t^e, w_{t-1}^e, \dots, w_{t-N_s}^e$  and there are  $2^{N_{in}}$  paths for the next state transitions (Viterbi, 1998). Consequently, the time- and space-complexity can be reduced to be  $\mathcal{O}(2^{N_{in} \cdot (N_s+1)} \cdot l)$  by dynamic programming that computes the maximum-likelihood sequence in

a hidden Markov model (Forney, 1973). For details of our encryption algorithm, the reader is referred to Appendix B.

**Lossless compression** Any random number generators cannot produce outputs perfectly matching all unpruned weights (i.e.,  $E$  is always less than 100%). To correct unmatched outputs of a random number generator (by flipping  $0 \leftrightarrow 1$ ) in order to enable lossless compression, the locations of all unmatched weight bits need to be recorded. Note that if  $E \approx 1$ , the number of unmatched weight bits is a lot smaller than the number of encrypted weight bits. If that is the case, such correction information can be stored in a separate on-chip memory that can be independently accessed without disturbing decryption operations. We propose a format representing such correction information in Appendix C where each unmatched weight bit requires  $N_c$  bits in the correction format ( $N_c$  is around 10 in Appendix C). Taking into account a compression ratio of a generator given as  $N_{out}/N_{in}$  and additional correction information (using  $N_c$  bits per one unmatched weight bit), a binary weight matrix  $\mathbf{W}^b \in \{0, 1\}^{m \times n}$  can be compressed into  $(\frac{N_{in}}{N_{out}}mn + N_{err})$  bits when  $N_{err} = N_c \times (\# \text{ of unmatched bits}) = N_c mn(1 - S)(1 - E)$ . Subsequently, memory reduction can be expressed as

$$\begin{aligned} \text{Mem. Save} &= 1 - ((N_{in}/N_{out})mn + N_{err})/(mn) \\ &= 1 - (1 - S)(1 + (1 - E)N_c), \end{aligned} \quad (3)$$

when  $N_{in}/N_{out}$  is given as  $(1 - S)$ . Thus, memory reduction approaches  $S$  when  $E$  approaches 1.

## 6. Experimental Results

In this section, we demonstrate the encryption capability of our proposed sequential encryption techniques using synthetic random data and NNs pruned by various pruning methods. Even though increasing  $N_{in}$  and  $N_s$  enhances  $E$ , to support dynamic programming technique (for sequential encryption) within 32GB memory of a single GPU,  $(N_{in} \times N_s)$  is empirically limited to be less than 26. For our experiments,  $N_{in}$  is selected to be 8 such that we feed a decryptor on a byte-level.

### 6.1. Synthetic Random Data ( $N_{in}=8$ )

**Setup** We generate a random weight 1-D vector of 1M bits (with equal amounts of zeros and ones). We also create a random masking data of 1M bits in which the percentage of zeros equals  $S$ .  $M^{\oplus}$  matrix (formulating the structure of an XOR-gate network) basically needs to be designed to maximize the randomness among outputs. Measuring randomness, however, is challenging and such measurement may not be highly correlated to  $E$ . Alternatively, we try numerous random  $M^{\oplus}$  matrices and choose a particular  $M^{\oplus}$  of the highest  $E$ . Specifically, for a given set of  $N_{in}$

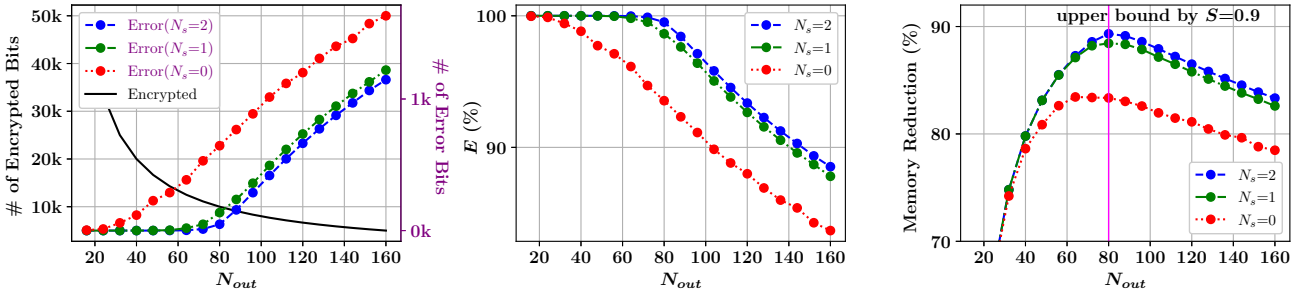


Figure 7. Impact of  $N_s$  on compression capability with various  $N_{out}$  using 1M random bits,  $N_{in} = 8$ , and  $S=0.9$ .

Table 1. Memory reduction (%) using 1M random bits and various  $N_s$  and  $S$  when  $N_{in} = 8$  and  $N_{out}=N_{in} \cdot 1/(1-S)$ .

$N_s \backslash S$	60.0%	70.0%	80.0%	90.0%
0	38.6%	53.8%	67.9%	83.5%
1	55.9%	67.4%	77.5%	88.5%
2	58.4%	69.1%	78.9%	89.3%

and  $N_{out}$ , an element of  $M^\oplus \in \mathbb{R}^{N_{out} \times ((N_s+1) \cdot N_{in})}$  is randomly assigned to 0 or 1 with equal probability. Then,  $E$  of those random  $M^\oplus$  matrices is estimated by using given random binary weight vectors and masking data. The best  $M^\oplus$  providing the highest  $E$  (for a given set of  $N_{in}$  and  $N_{out}$ ) is then utilized for our experiments.

**Compression capability** Figure 7 demonstrates the impact of  $N_s$  on  $E$  and corresponding memory reduction(%) with various  $N_{out}$  and 1M random bits when  $N_{in}=8$  and  $S=0.9$ . Regardless of  $N_s$ , as  $N_{out}$  increases (i.e., the compression ratio ( $=N_{out}/N_{in}=N_{out}/8$ ) of a decryptor increases), the number of encrypted bits is reduced while the number of unmatched (error) bits increases. Because of such a trade-off between the number of encrypted bits and the number of error bits, there exists a certain  $N_{out}$  that maximizes the memory reduction. Note that compared to a non-sequential encryption (of  $N_s=0$ ), sequential encryption (even with small  $N_s$ ) significantly reduces the number of error bits and maintains high  $E$  (of almost 100%) until  $N_{out}$  reaches  $N_{in} \times (1/(1-S))=80$ . Indeed, memory reduction becomes highest ( $=89.32\%$ ) when  $N_s$  is highest and  $N_{out}$  is 80 in Figure 7. As we discussed for lossless compression in Section 5, 89.32% of memory reduction is close to  $S(=90\%)$  that is the maximum memory reduction obtained when  $E \approx 1$ . In the remainder of this paper,  $N_{out}$  is given as  $N_{in} \times (1/(1-S))$  to maximize the memory reduction.

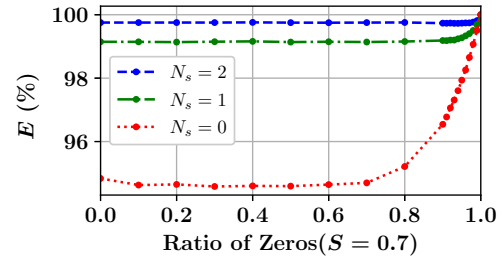


Figure 8.  $E$  with various ratio of zero in a random vector when  $S=0.7$  and  $N_s=0, 1$ , or 2.

**Impact of  $S$  on memory reduction** Table 1 presents memory reduction using various  $S$ . Note that for a certain  $S$  in Table 1, as  $N_s$  increases, the difference between  $S$  and memory reduction decreases. In other words, regardless of  $S$ , sequential encryption/decryption principles are crucial for memory reduction to approach  $S$  which is the maximum. Increasing  $S$  also facilitates memory reduction to approach  $S$  in Table 1 as described in Eq. 3 where increasing  $S$  with a constant  $E$  enhances memory reduction.

**Inverting technique** So far, we assumed that a binary weight matrix holds equal amounts of zeros and ones. A few representations such as binary-coding-based quantization (Rastegari et al., 2016; Xu et al., 2018) and signed INT8 (Jacob et al., 2018) would inherently justify such an assumption. However, there exist exceptional representations as well (e.g., FP32 in which exponent bits incorporate lots of zeros). We conduct experiments to find a relationship between the ratio of zeros and  $E$  using a random weight vector as shown in Figure 8.  $E$  increases if a substantial amount of zeros are employed as unpruned weight bits, because of a higher chance to find trivial inputs (of all zeros fed into XOR operations) to produce zero outputs. Hence, to improve  $E$  (especially when  $N_s$  is low), we propose an inverting technique where an entire binary weight vector is inverted if the ratio of zeros is less than 50%.

Table 2.  $E$  and memory reduction of sparse Transformer and ResNet-50 pruned by two different pruning methods. For  $N_s=0$  and  $N_s=1$ , inverting technique is selectively applied to a layer if unpruned weights in such a layer accommodate more zeros than ones. Inverting has no effect when weights are represented by signed INT8.

MODEL	$S$	PRUNING METHOD	$E$ (%) (MAX: 100%)			MEMORY REDUCTION (%) (MAX: $S$ )		
			NON-SEQ. $N_s=0$ (INV.)	SEQUENTIAL $N_s=1$ (INV.)	$N_s=2$	NON-SEQ. $N_s=0$ (INV.)	SEQUENTIAL $N_s=1$ (INV.)	$N_s=2$
TRANSFORMER on WMT'14 en-de (FP32)	70%	MAGNITUDE	93.8(94.5)	98.0(98.3)	<b>98.7</b>	50.3(52.4)	63.1(63.8)	<b>65.3</b>
		RANDOM	94.6(95.2)	99.2(99.3)	<b>99.8</b>	52.8(54.6)	66.6(66.8)	<b>68.3</b>
	90%	MAGNITUDE	92.6(93.9)	97.6(97.9)	<b>98.4</b>	82.4(83.7)	87.4(87.7)	<b>88.2</b>
		RANDOM	93.7(94.5)	98.7(98.9)	<b>99.5</b>	83.5(84.3)	88.5(88.7)	<b>89.3</b>
RESNET-50 on ImageNet (FP32)	70%	MAGNITUDE	94.4(95.0)	98.6(98.7)	<b>99.1</b>	52.2(54.2)	64.7(65.3)	<b>66.5</b>
		RANDOM	94.6(95.1)	99.1(99.2)	<b>99.7</b>	52.7(54.2)	66.5(66.7)	<b>68.3</b>
	90%	MAGNITUDE	92.7(93.7)	97.3(97.6)	<b>98.1</b>	82.5(83.5)	87.1(87.4)	<b>87.9</b>
		RANDOM	92.7(93.5)	97.6(97.9)	<b>98.7</b>	82.5(83.3)	87.5(87.7)	<b>88.6</b>
RESNET-50 on ImageNet (SIGNED INT8)	70%	MAGNITUDE	93.9(N/A)	98.5(N/A)	<b>99.1</b>	50.9(N/A)	64.5(N/A)	<b>66.4</b>
		RANDOM	96.2(N/A)	99.7(N/A)	<b>99.9</b>	57.6(N/A)	68.3(N/A)	<b>69.0</b>
	90%	MAGNITUDE	92.4(N/A)	97.1(N/A)	<b>98.0</b>	82.2(N/A)	86.9(N/A)	<b>87.8</b>
		RANDOM	93.5(N/A)	98.2(N/A)	<b>99.2</b>	83.3(N/A)	88.0(N/A)	<b>89.0</b>

Table 3. Coefficient of variation of  $n_u$  and  $E$  of two selected layers of the Transformer pruned by random, magnitude-based, or L0 regularization pruning method.

PRUNING METHOD	TARGET $S$	LAYER: DEC3/SELF-ATT/Q (512 × 512), FP32				LAYER: DEC3/FFN2 (2048 × 512), FP32			
		COEFF. OF VARIATION ( $n_u$ )	$E$ (%)			COEFF. OF VARIATION ( $n_u$ )	$E$ (%)		
			$N_s=0$	$N_s=1$	$N_s=2$		$N_s=0$	$N_s=1$	$N_s=2$
RANDOM	0.7	0.299	94.6	99.2	<b>99.8</b>	0.303	94.6	99.2	<b>99.8</b>
MAGNITUDE		0.324	94.5	98.9	<b>99.6</b>	0.366	94.1	98.3	<b>98.9</b>
L0 REG.		0.347	94.5	99.0	<b>99.6</b>	0.331	94.3	98.7	<b>99.2</b>

## 6.2. Sparse Transformer and ResNet-50 ( $N_{in}=8$ )

We measure compression capability of our proposed sequential encryption scheme using sparse Transformer (Vaswani et al., 2017) on WMT'14 en-de dataset and ResNet-50 (He et al., 2016) on ImageNet. Those two models<sup>1</sup> in FP32 format are pruned by various methods including magnitude-based one (Han et al., 2015), L0 regularization (Louizos et al., 2018), and random pruning (Gale et al., 2019) (also variational dropout (Molchanov et al., 2017) in Appendix D). For the ResNet-50 model (on ImageNet), we also consider signed INT8 format (Jacob et al., 2018).

Table 2 presents  $E$  and memory reduction when every layer of the Transformer and ResNet-50 is pruned by the same pruning rate  $S$ . Both  $E$  and memory reduction are significantly improved by increasing  $N_s$ . Even compared to the case when inverting technique is applied to non-sequential encryption ( $N_s=0$ ), we observe that sequential encryption ( $N_s>0$ ) without inverting yields a lot higher compression capability (inverting technique provides a minor improvement on sequential encryption scheme). Note that the compression capability difference between random pruning and

magnitude-based pruning methods are similar in Table 2 such that our experiments with synthetic random data are justified. Such justification is also verified in Table 3 that is achieved by using two selected layers of the Transformer. Compared to random pruning, magnitude-based and L0 regularization pruning methods exhibit somewhat lower  $E$  that is related to higher coefficients of variation of  $n_u$ . See Appendix D for additional results.

All in all, our proposed sequential encryption method designed in the context of random pruning is also effective for other fine-grained pruning methods. Through various cases including synthetic data and benchmark models, we demonstrated the superiority of the proposed sequential encryption scheme to previous fixed-to-fixed compression methods including a non-sequential XOR-gate network of  $N_s=0$  (Kwon et al., 2020) and a Viterbi-based encoder structure where  $N_{in}$  is limited to be 1 (Ahn et al., 2019).

## 7. Conclusion

In this paper, we proposed a sequential encryption scheme that is a useful fixed-to-fixed compression for sparse NNs. We studied the maximum compression ratio using entropy based on the strategy of mapping a weight block into a

<sup>1</sup>[https://github.com/google-research/google-research/tree/master/state\\_of\\_sparsity](https://github.com/google-research/google-research/tree/master/state_of_sparsity)



small number of symbols. We also investigated random number generators as a practical fixed-to-fixed decryptor using an XOR-gate network. Random number generators can improve compression capability if input vectors are reused for multiple time indices through shift registers. Throughout various synthetic random data and benchmark models, we demonstrated that our proposed sequential encryption scheme can achieve almost the maximum compression ratio.

## References

- Ahn, D., Lee, D., Kim, T., and Kim, J.-J. Double Viterbi: Weight encoding for high compression ratio and fast on-chip reconstruction for deep neural network. In *International Conference on Learning Representations (ICLR)*, 2019.
- Forney, G. D. The Viterbi algorithm. *Proc. of the IEEE*, 61: 268 – 278, March 1973.
- Frankle, J. and Carbin, M. The lottery ticket hypothesis: Finding sparse, trainable neural networks. *arXiv:1803.03635*, 2018.
- Gale, T., Elsen, E., and Hooker, S. The state of sparsity in deep neural networks. *arXiv preprint arXiv:1902.09574*, 2019.
- Gale, T., Zaharia, M., Young, C., and Elsen, E. Sparse gpu kernels for deep learning. *arXiv preprint arXiv:2006.10901*, 2020.
- Golomb, S. Run-length encodings. *IEEE Transactions on Information Theory*, 12(3):399–401, 1966.
- Han, S., Pool, J., Tran, J., and Dally, W. J. Learning both weights and connections for efficient neural networks. In *Advances in Neural Information Processing Systems*, pp. 1135–1143, 2015.
- He, K., Zhang, X., Ren, S., and Sun, J. Deep residual learning for image recognition. *2016 IEEE Conference on Computer Vision and Pattern Recognition (CVPR)*, pp. 770–778, 2016.
- He, Y., Zhang, X., and Sun, J. Channel pruning for accelerating very deep neural networks. In *Proceedings of the IEEE International Conference on Computer Vision*, pp. 1389–1397, 2017.
- Huffman, D. A. A method for the construction of minimum-redundancy codes. *Proceedings of the IRE*, 40(9):1098–1101, 1952.
- Jacob, B., Kligys, S., Chen, B., Zhu, M., Tang, M., Howard, A., Adam, H., and Kalenichenko, D. Quantization and training of neural networks for efficient integer-arithmetic-only inference. In *Proceedings of the IEEE Conference on Computer Vision and Pattern Recognition*, pp. 2704–2713, 2018.
- Kwon, S. J., Lee, D., Kim, B., Kapoor, P., Park, B., and Wei, G.-Y. Structured compression by weight encryption for unstructured pruning and quantization. In *Proceedings of the IEEE/CVF Conference on Computer Vision and Pattern Recognition*, pp. 1909–1918, 2020.
- LeCun, Y., Denker, J. S., and Solla, S. A. Optimal brain damage. In *Advances in Neural Information Processing Systems*, pp. 598–605, 1990.
- Lee, D., Kwon, S. J., Kapoor, P., Kim, B., and Wei, G.-Y. Network pruning for low-rank binary indexing. *arXiv:1905.05686*, 2019a.
- Lee, N., Ajanthan, T., and Torr, P. H. Snip: Single-shot network pruning based on connection sensitivity. In *ICLR*, 2019b.
- Li, H., Kadav, A., Durdanovic, I., Samet, H., and Graf, H. P. Pruning filters for efficient convnets. In *International Conference on Learning Representations*, 2017.
- Liu, Z., Li, J., Shen, Z., Huang, G., Yan, S., and Zhang, C. Learning efficient convolutional networks through network slimming. In *ICCV*, 2017.
- Louizos, C., Welling, M., and Kingma, D. P. Learning sparse neural networks through l<sub>0</sub> regularization. In *International Conference on Learning Representations*, 2018. URL <https://openreview.net/forum?id=H1Y8hhg0b>.
- Molchanov, D., Ashukha, A., and Vetrov, D. P. Variational dropout sparsifies deep neural networks. In *International Conference on Machine Learning (ICML)*, pp. 2498–2507, 2017.
- Morelos-Zaragoza, R. H. *The art of error correcting coding*. John Wiley & Sons, 2nd edition, 2006.
- Narang, S., Diamos, G., Sengupta, S., and Elsen, E. Exploring sparsity in recurrent neural networks. In *International Conference on Learning Representations (ICLR)*, 2017.
- Rastegari, M., Ordonez, V., Redmon, J., and Farhadi, A. XNOR-Net: Imagenet classification using binary convolutional neural networks. In *ECCV*, 2016.
- Renda, A., Frankle, J., and Carbin, M. Comparing rewinding and fine-tuning in neural network pruning. *arXiv preprint arXiv:2003.02389*, 2020.
- Vaswani, A., Shazeer, N., Parmar, N., Uszkoreit, J., Jones, L., Gomez, A. N., Kaiser, L., and Polosukhin, I. Attention is all you need. *arXiv:1706.03762*, 2017.

- Viterbi, A. J. An intuitive justification and a simplified implementation of the map decoder for convolutional codes. *IEEE Journal on Selected Areas in Communications*, 16(2):260–264, 1998.
- Wang, C., Zhang, G., and Grosse, R. Picking winning tickets before training by preserving gradient flow. In *International Conference on Learning Representations*, 2020. URL <https://openreview.net/forum?id=SkgsACVKPH>.
- Xu, C., Yao, J., Lin, Z., Ou, W., Cao, Y., Wang, Z., and Zha, H. Alternating multi-bit quantization for recurrent neural networks. In *International Conference on Learning Representations (ICLR)*, 2018.
- Yu, J., Lukefahr, A., Palframan, D., Dasika, G., Das, R., and Mahlke, S. Scalpel: Customizing DNN pruning to the underlying hardware parallelism. In *Proceedings of the 44th Annual International Symposium on Computer Architecture*, pp. 548–560, 2017.
- Zhou, A., Ma, Y., Zhu, J., Liu, J., Zhang, Z., Yuan, K., Sun, W., and Li, H. Learning n:m fine-grained structured sparse neural networks from scratch. In *International Conference on Learning Representations*, 2021. URL [https://openreview.net/forum?id=K9bw7vqp\\_s](https://openreview.net/forum?id=K9bw7vqp_s).
- Zhu, M. and Gupta, S. To prune, or not to prune: exploring the efficacy of pruning for model compression. *CoRR*, abs/1710.01878, 2017.
- Ziv, J. and Lempel, A. Compression of individual sequences via variable-rate coding. *IEEE Transactions on Information Theory*, 24(5):530–536, 2006.

## A. Performance of Sparse Matrix Multiplication using CSR Format

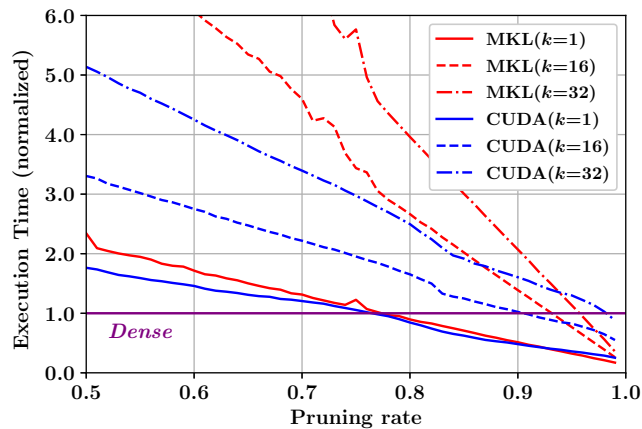


Figure S.9. Normalized execution time of multiplying a  $(2048 \times 2048)$  sparse matrix with a  $(2048 \times k)$  dense matrix.

For inference of NNs, it is known that performance (including latency and throughput) is dominated by matrix multiplications. Figure S.9 presents performance when a  $(2048 \times 2048)$  sparse matrix (of CSR format) is multiplied by a  $(2048 \times k)$  dense matrix when  $k$  is usually small for inference with small batch size. MKL library (operated by i7-7700 @ 3.6GHz) and CUDA 10.2 library (performed by nVIDIA V100) perform sparse matrix multiplications whose execution times are normalized with respect to corresponding dense matrix multiplications (i.e., using a dense  $(2048 \times 2048)$  matrix). From Figure S.9, it should be noted that even with a high compression ratio (due to high pruning rate), if CSR format is adopted, sparse matrix multiplications can be even slower than dense matrix multiplication. Thus, proposing a regular format after fine-grained pruning is critical for parallel computing to achieve performance gain by pruning.

## B. Encryption Algorithm

In this section, we describe our encryption algorithm based on dynamic programming algorithm. For each binary weight  $\mathbf{W}_i^b$  ( $0 \leq i \leq n_w$ ), the function ENCRYPTION generates the encrypted vectors  $w_{i,(1..l+N_s)}$ . XOR-gate networks ( $\mathbf{M}^\oplus$ ) are pre-determined and fixed for inference. Note that the number of encrypted vectors ( $\mathbf{w}_{1..(l+N_s)}^e$ ) is  $l + N_s$ , not  $l$ .  $w_1^e$  and  $w_2^e$  are pre-determined as  $\text{BIN}(0)$  and used for encrypting the first binary weight vector.

**Algorithm 1** Encryption algorithm when  $N_s = 2$ . For a binary matrix  $\mathbf{W}_i^b$ , the ENCRYPTION function generates encrypted bit vectors. For varied  $N_s$ , the number of for-loop statements for  $i^t$  (e.g. line 34-36) and the dimensions of arrays ( $dp$  and  $path$ ) are changed to  $N_s + 1$ .

```

1: Parameters
2:    $\mathbf{W}_i^b$  : Binary weights to be encrypted
3:    $MASK$  : Pruning masks for  $\mathbf{W}_i^b$ 
4:    $dp$  : ( $N_s+1$ )-dimensional array.  $dp[t][a][b]$  stores
   the minimum number of error bits when  $\text{BIN}(a)$  and
    $\text{BIN}(b)$  are fixed as  $w_t^e$  and  $w_{t-1}^e$ .
5:    $path$  : ( $N_s+1$ )-dimensional array for history
6: Functions
7:    $\text{SIZE}(\mathbf{W})$  returns the number of parameters in  $\mathbf{W}$ .
8:    $\text{RESHAPE}(ar, shape)$  returns same data ( $ar$ ) with
   specified shape,  $shape$ .
9:    $\text{INIT}(ar, init)$  sets a value  $init$  to all elements in  $ar$ .
10:   $\text{BIN}(dec)$  returns a binary value of  $dec$ .
11:   $\text{DEC}(bin)$  returns a decimal value of  $bin$ .
12:
13: function ERR_NUM( $x, y, mask$ )
14:    $nErr \leftarrow 0$ 
15:   for  $i \leftarrow 0$  to  $N_{out} - 1$  do
16:     if  $mask[i] \neq 0$  and  $x[i] \neq y[i]$  then
17:        $nErr \leftarrow nErr + 1$ 
18:     end if
19:   end for
20:   return  $nErr$ 
21: end function
22:
23: function ENCRYPTION( $\mathbf{W}_i^b, MASK$ )
24:    $l \leftarrow \text{SIZE}(\mathbf{W}_i^b)/N_{out}$ 
25:    $data \leftarrow \text{RESHAPE}(\mathbf{W}_i^b, [l, N_{out}])$   $\triangleright$  Slicing
26:    $mask \leftarrow \text{RESHAPE}(MASK, [l, N_{out}])$   $\triangleright$  Slicing
27:    $\text{INIT}(dp, INF)$   $\triangleright$  Initialize for starting point
28:    $dp[N_s][0][0] \leftarrow 0$ .
29:    $w_1^e, w_2^e \leftarrow \text{BIN}(0), \text{BIN}(0)$ 
30:
31:   /* Find the minimum number of errors */
32:   for  $t \leftarrow N_s+1$  to  $l+N_s$  do
33:     for  $i^t \leftarrow 0$  to  $2^{N_{in}}-1$  do
34:       for  $i^{t-1} \leftarrow 0$  to  $2^{N_{in}}-1$  do
35:         for  $i^{t-2} \leftarrow 0$  to  $2^{N_{in}}-1$  do
36:            $out \leftarrow \mathbf{M}^\oplus(\text{BIN}(i^{t-2}) \frown \text{BIN}(i^{t-1}) \frown \text{BIN}(i^t))$ 
37:            $n_{err} \leftarrow \text{ERR\_NUM}(out, data[t], mask[t])$ 
38:           if  $dp[t][i^t][i^{t-1}] > n_{err} +$ 
39:              $dp[t-1][i^{t-1}][i^{t-2}]$  then
40:                $dp[t][i^t][i^{t-1}] \leftarrow n_{err} + dp[t -$ 
41:                  $1][i^{t-1}][i^{t-2}]$ 
42:                $path[t][i^t][i^{t-1}] \leftarrow \text{BIN}(i^{t-2})$ 
43:             end if
44:           end for
45:         end for
46:       end for
47:     /* Find the last two(= $N_s$ ) encrypted vectors */
48:      $min_{err} \leftarrow INF$ .
49:     for  $i^t = 0$  to  $2^{N_{in}} - 1$  do
50:       for  $i^{t-1} = 0$  to  $2^{N_{in}} - 1$  do
51:         if  $min_{err} > dp[l + N_s][i^t][i^{t-1}]$  then
52:            $min_{err} \leftarrow dp[l + N_s][i^t][i^{t-1}]$ 
53:            $w_{l+2}^e, w_{l+1}^e \leftarrow \text{BIN}(i^{t-1}), \text{BIN}(i^t)$ 
54:         end if
55:       end for
56:     /* Get encrypted bits by following history array */
57:     for  $t \leftarrow l$  to  $2N_s + 1$  by  $-1$  do
58:        $w_t^e \leftarrow path[t + N_s][\text{DEC}(w_{t+2}^e)][\text{DEC}(w_{t+1}^e)]$ 
59:     end for
60:     return  $\{w_1^e, w_2^e, \dots, w_{l+N_s}^e\}$ 
61:   end function
62:

```



### C. Memory Reduction with Lossless Compression

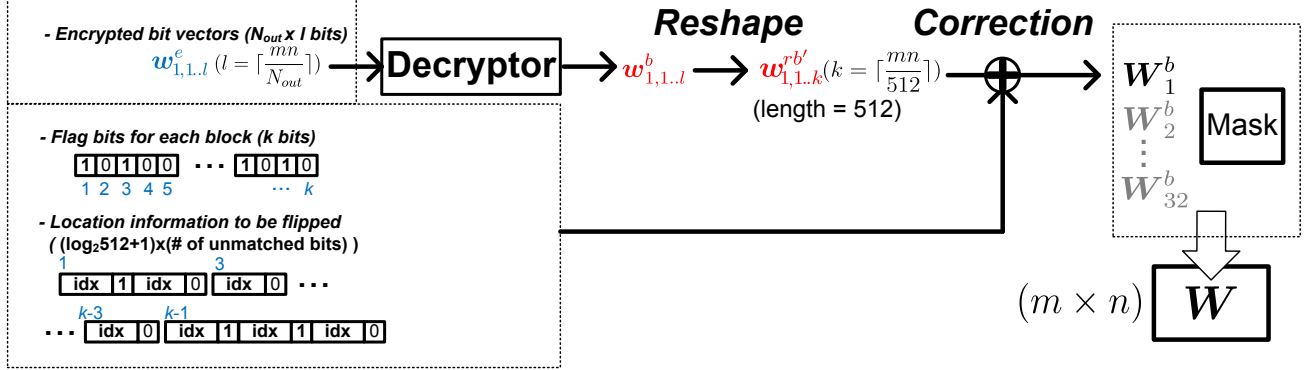


Figure S.10. Correction process for lossless compression. After the encrypted (compressed) bit vectors are decrypted, unmatched bits (that encryption could not target successfully) are flipped by correction information that records the locations of unmatched weight bits.

For lossless compression, the unmatched bits (error bits) should be corrected right after decryption procedures. Since the random number generator produces 0 or 1, the unmatched bits can be simply corrected by flipping.

To compute the memory reduction, we suggest block-wise correction logic to be conducted by flipping error bits in a  $p$ -length vector while each error location is given as a bit position inside a vector. As depicted in Figure S.10, when the block-wise correction is performed while a block size has  $p$ -length, the decrypted vectors  $w_{1..l}^b$  are reshaped to  $w_{1..k}^{r,b'}$  ( $k = \lceil \frac{mn}{p} \rceil$ ) and each reshaped vector  $w^{r,b'}$  is corrected by corresponding error bit locations indicating which bit is to be flipped inside a block (of  $p$ -length).

The amount of compressed bits can be computed as

$$N_{in} \cdot \lceil \frac{mn}{N_{out}} \rceil + \lceil \frac{mn}{p} \rceil + (\log_2 p + 1) \times (\# \text{ of unmatched bits}). \quad (4)$$

The first term is the number of bits of  $w_{1..l}^e$  as the compression results by sequential encryption. The second term is the number of flag bits while each flag bit indicates whether a non-zero number of unmatched bits exists in each  $p$ -length vector (as  $E$  approaches 1, there are many  $p$ -length vectors that skip the correction step). The third term includes locations of unmatched bits (inside a  $p$ -length block) to be flipped and an additional one bit to specify the end of the streaming error bit locations (i.e., '1' means the following  $(\log_2 p)$  bits contains the next correction information of the same block). Thus, each block of  $p$ -length involves  $(\log_2 512 + 1) \times (\# \text{ of unmatched bits})$  for error bit locations.

## D. Additional Analysis on Experiments

In this section, we provide additional analysis and results for experiments in Section 6.2.

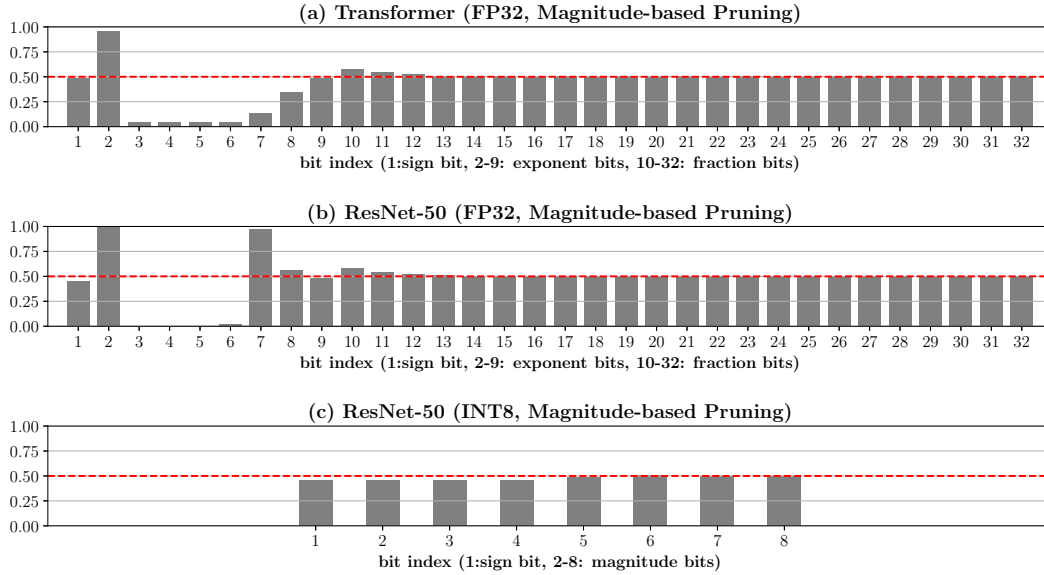


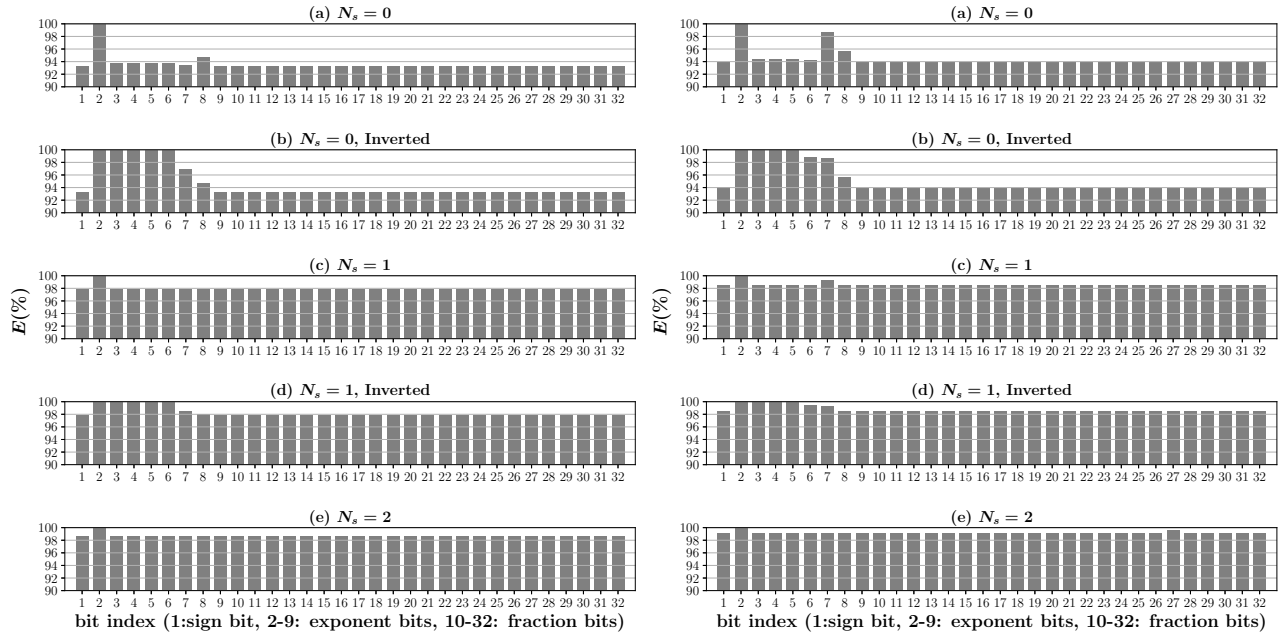
Figure S.11. Ratio of zeros when weights are divided into  $k$  groups when  $k$  is the bit-index (i.e., for FP32 number format,  $k=1$  means a sign bit and  $k=32$  means the least significant bit in mantissa). For models, Transformer(FP32), ResNet-50(FP32), and ResNet-50(INT8) are investigated. Most weights consist of similar amounts of 0s and 1s. For the exponent bits of FP32 models, there are noticeable skewed ratios of zeros (e.g. while most of the 2<sup>nd</sup> bits in Transformer are zero, most of 3<sup>rd</sup>, 4<sup>th</sup>, and 5<sup>th</sup> bits are ones.) because the range of exponent bits is limited according to characteristics of DNN models (e.g. regularization such as weight decay). We can gain additional efficiency by adopting the inverting technique for the FP32 models.

Table S.4. Coefficient of variation of  $n_u$  and  $E$  of selected layers of the Transformer pruned by random, magnitude-based, L0 regularization, or variational dropout pruning method.

$N_{in}, N_{out}$	SHAPE	$S$	LAYER NAME	PRUNING METHOD	COEFF	$E$ (%)		
						$N_s=0$	$N_s=1$	$N_s=2$
(8, 26)	(512, 512)	0.700	DEC3/SELF_ATT/Q	RANDOM	0.341	93.7%	98.7%	99.5%
	(2048, 512)	0.700	DEC3/FFN2	RANDOM	0.343	93.7%	98.7%	99.5%
	(512, 512)	0.700	DEC3/SELF_ATT/Q	MAGNITUDE	0.390	93.4%	98.2%	99.0%
	(2048, 512)	0.700	DEC3/FFN2	MAGNITUDE	0.363	93.6%	98.5%	99.2%
	(512, 512)	0.699	DEC3/SELF_ATT/Q	L0 REG.	0.476	92.7%	97.6%	98.7%
	(512, 512)	0.698	DEC3/FFN2	L0 REG.	0.467	92.7%	97.7%	98.8%
	(512, 512)	0.705	DEC5/SELF_ATT/K	VAR. DROPOUT	0.303	94.5%	99.1%	99.7%
	(2048, 512)	0.697	DEC1/FFN1	VAR. DROPOUT	0.309	94.5%	99.1%	99.7%
(8, 80)	(512, 512)	0.900	ENC2/SELF_ATT/OUTPUT	RANDOM	0.349	94.4%	98.6%	99.3%
	(2048, 512)	0.900	DEC5/FFN2	RANDOM	0.315	94.6%	98.9%	99.5%
	(512, 512)	0.900	ENC2/SELF_ATT/OUTPUT	MAGNITUDE	0.516	92.5%	97.0%	98.0%
	(2048, 512)	0.900	DEC5/FFN2	MAGNITUDE	0.363	93.7%	98.5%	99.1%
	(512, 512)	0.904	ENC2/SELF_ATT/OUTPUT	L0 REG.	0.331	94.3%	98.7%	99.2%
	(512, 512)	0.896	DEC5/FFN2	L0 REG.	0.347	94.5%	99.0%	99.6%
	(512, 512)	0.906	DEC2/SELF_ATT/V	VAR. DROPOUT	0.770	89.4%	93.6%	94.3%
	(2048, 512)	0.904	DEC4/FFN1	VAR. DROPOUT	0.499	91.8%	96.4%	97.4%

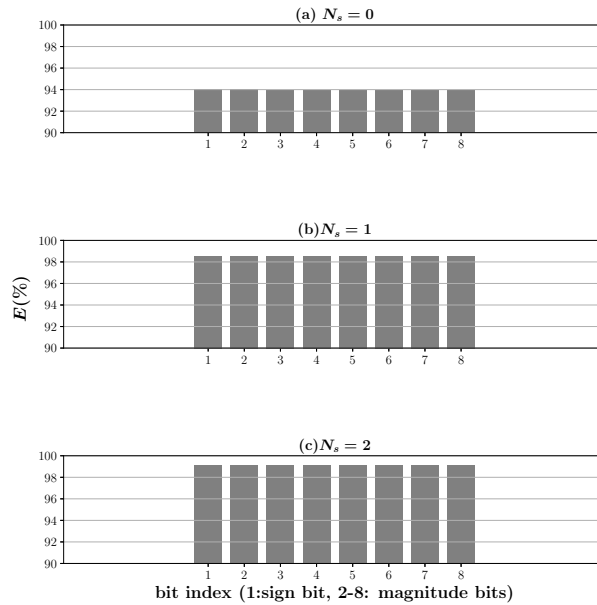
 Table S.5. Coefficient of variation of  $n_u$  and  $E$  of selected layers of the ResNet-50 pruned by random, magnitude-based, or variational dropout pruning method.

$N_{in}, N_{out}$	SHAPE	$S$	LAYER NAME	PRUNING METHOD	COEFF	$E$ (%)		
						$N_s=0$	$N_s=1$	$N_s=2$
(8, 26)	(1,1,1024,256)	0.700	GROUP2_LAYER3_BN2	RANDOM	0.347	94.2%	98.6%	99.2%
	(1,1,256,1024)	0.700	GROUP3_LAYER5_BN3	RANDOM	0.334	94.3%	98.8%	99.5%
	(1,1,1024,256)	0.700	GROUP2_LAYER3_BN2	MAGNITUDE	0.505	93.2%	98.0%	98.9%
	(1,1,256,1024)	0.700	GROUP3_LAYER5_BN3	MAGNITUDE	0.428	93.8%	98.4%	99.0%
	(3,3,512,512)	0.709	GROUP2_LAYER3_BN2	VAR. DROPOUT	0.403	94.2%	98.4%	99.1%
	(1,1,256,1024)	0.706	GROUP3_LAYER5_BN3	VAR. DROPOUT	0.361	94.4%	98.6%	99.1%
(8, 80)	(3, 3, 256, 256)	0.900	GROUP3_LAYER3_BN2	RANDOM	0.683	92.3%	96.8%	98.0%
	(1, 1, 512, 2048)	0.900	GROUP4_LAYER0_BN3	RANDOM	0.407	92.9%	97.4%	98.1%
	(3, 3, 256, 256)	0.900	GROUP3_LAYER3_BN2	MAGNITUDE	0.303	94.6%	99.2%	99.8%
	(1, 1, 512, 2048)	0.900	GROUP4_LAYER0_BN3	MAGNITUDE	0.299	94.6%	99.2%	99.8%
	(3, 3, 256, 256)	0.913	GROUP3_LAYER3_BN2	VAR. DROPOUT	0.366	94.1%	98.3%	98.9%
	(1, 1, 512, 2048)	0.896	GROUP4_LAYER0_BN3	VAR. DROPOUT	0.324	94.5%	98.9%	99.6%



(a) Transformer (FP32, Magnitude-based Pruning)

(b) ResNet-50 (FP32, Magnitude-based Pruning)



(c) ResNet-50 (INT8, Magnitude-based Pruning)

Figure S.12.  $E$  of the Transformer and ResNet-50 (pruned by  $S=70\%$ ) measured for each bit index ( $\leq 32$  for FP32) individually with various  $N_s$  while inverting technique is also considered. It can be observed that the inverting technique improves  $E$  for  $N_s = 0$  and  $N_s = 1$ . When  $N_s = 2$ , the improvement on  $E$  is not noticeable.